ADVANCED MATERIALS TECHNOLOGIES
www.advmattechnol.de

Next Generation of 3D-Printed Electronics: Electroplating Inside Channels to Embed 3D Copper Features within Polymeric Structures Fabricated Through Material Extrusion

Gianni Stano, Mattia D'Orazio, Antonio Pavone, and Gianluca Percoco*

Material Extrusion (MEX) 3D printing has been largely employed to process electrically conductive polymers to fabricate electronic components, which still suffer from bad performance due to high electrical resistance. The electroplating process is proven to drastically reduce the resistance by depositing a thin layer of copper on top of the electrically conductive polymer; however, this method comes with a price to pay: only external features can be plated with copper. The present research paper presents an innovative solution to overcome this issue by performing electroplating inside 3D-printed parts to plate internal layers (inaccessible for electroplating purposes with traditional approaches) with copper. Electroplating inside closed channels is performed: a remarkable reduction in electrical resistance of 5 orders of magnitude (from 2300 up to 0.08 Ω) is achieved in internal tracks. The proposed approach has also been implemented "on board" a commercial MEX machine to fabricate an assembly-free smart structure with a copper sensor completely embedded within dielectric material (improved performance compared to traditional counterpart). Furthermore, the proposed approach is proven to fully plate with copper not only planar tracks but also embedded 3D features such as coils. The present research unlocks the fabrication of assembly-free functional devices with embedded copper elements by only extruding polymers through MEX Additive Manufacturing.

1. Introduction

Material Extrusion (MEX) (ISO/ASTM 52900:2015), has emerged as one of the most flexible Additive Manufacturing technologies for the fabrication of functional devices,[1–3] as several materials can be processed at the same time, in the same fabrication cycle. Among all the materials, electrically conductive polymers result to be extremely appealing because they can be directly employed to fabricate sensors.[4–8] The fabrication of smart structures, composed of dielectric materials, and electrically conductive polymers has gained the interest of the additive manufacturing community, as structures with sensors capable of detecting different inputs can be additively manufactured via MEX with no assembly steps.[9–12]

Different areas related to the leverage of MEX for the manufacture of sensors have been investigated and intensively studied, spanning from i) electrically conductive polymer formulation, ii) 3D printing setup, and iii) 3D-printed sensors. Sun et al[13] developed a custom-made silver-filled filament based on a thermoplastic polyurethane (TPU) matrix. The proposed filament results in good printability due to the addition of plasticizer, and it is characterized by high conductivity (because of the silver filler) and good flexibility (TPU matrix): it was proven to maintain electrical performance up to 60% of strain, resulting appealing for the fabrication of stretchable devices. Hernandez et al[6] developed a carbon nanofiber (CNF)- filled polylactic acid (PLA) filament, investigating the relationship among process parameters, wt% of CNF, and sensitivity of 3D-printed sensors, finding an optimal configuration allowing the manufacturing of low-cost strain sensors. Mohammadi et al[14] developed a recyclable paste composed of graphite and cellulose nanocrystal powder for MEX systems: a direct correlation between cellulose wt% and compression strength was found, as well as superior electrical properties (conductivity of 2400 S/m) compared to other graphite materials for MEX.

From a 3D printing MEX machine standpoint, recent works tackled the problem of non-planar and conformal sensor fabrication: Hong et al[15] proposed a 5-axis robotic system to extrude conductive polylactic acid (CPLA), proving that a conformal approach improves the conductivity of extruded tracks compared to traditional planar 3D printing because of the improved inter-layer adhesion. Similarly, Emon et al[16] recurred to a

G. Stano, M. D'Orazio, A. Pavone, G. Percoco
Department of Mechanics, Mathematic and Management Engineering (DMMM)
Polytechnic University of Bari
Via E. Orabona 4, Bari 70125, Italy
E-mail: gianni.stano@poliba.it
G. Stano, M. D'Orazio, A. Pavone, G. Percoco
Interdisciplinary Additive Manufacturing (IAM) Lab
Polytechnic University of Bari
Viale del Turismo 8, Taranto 74100, Italy

The ORCID identification number(s) for the author(s) of this article can be found under https://doi.org/10.1002/admt.202401923

DOI: 10.1002/admt.202401923

curved substrate to conformally extrude a pressure sensor, which was benchmarked with its counterpart (planar-based) showing higher sensitivity and less hysteresis. Marion et al[17] studied the clogging issue negatively affecting the extrusion of electrically conductive polymers; they developed a novel nozzle (driven by fluid dynamics simulations) to prevent clogging, thereby resulting in improved electrical performance of the extruded CPLA (conductivity increased up to 42%) as the porosity is reduced too.

From a 3D-printed sensor standpoint, several research works have been carried out, demonstrating that sensors belonging to three main classes, based on their working principle, can be fabricated: piezoresistive,[18–22] capacitive,[23–25] and piezoelectric.[26] It should be said that also a combination of the above-mentioned sensors can be monolithically fabricated and integrated into 3D-printed structures: as demonstrated in,[27] a soft robotic finger with embedded piezoresistive-based, and capacitive-based sensors was manufactured with no assembly steps.

Some of the major benefits coming from the leverage of MEX for the fabrication of sensors are: wearability, reduction of assembly steps, cost-effectiveness, time-saving, fabrication of complex geometries, and embedding of sensors within dielectric structures.[28,29]

However, the main limitation of the MEX approach is related to the usage of electrically conductive polymers. Because of their internal composition (polymer doped with conductive filler), and their conductive mechanism (percolation theory),[30] electrically conductive polymers suffer from low electrical properties compared to traditional conductors (i.e., copper) due to their high electrical resistance (low conductivity).

At the state of the art, the most effective approach to greatly reduce the electrical resistance of 3D-printed sensors is based on plating the extruded electrically conductive polymer with a thin layer of metals (i.e., copper) by recurring to metallization post-processing, such as electroplating and electroless plating. The main difference between the two metallization techniques is that the electroplating process requires electrical current to make the metal ions (generally copper) move from the anode to the cathode (3D-printed part to be plated); while the electroless plating only relies on a reducing agent (no electrical current is needed) to coat 3D-printed conductive parts with metal. Several research works demonstrated the effectiveness of both electroplating,[31–33] and electroless plating[34–36] to improve conductivity in sensors manufactured via MEX. Angel et al.,[31] demonstrated that complex electronic elements such as inductors can be fabricated with easy via MEX, and subsequentially post-processed by recurring to the electroplating technique to greatly reduce the electrical resistance of 5 orders of magnitude. The electroplating technique was leveraged by Lazarus et al[33] to selectively plate with copper multiple tracks extruded on top of dielectric PLA, in order to create circuits including external elements soldered over electroplated tracks. Other variables related to the electroplating process applied to 3D-printed parts have been studied, such as the relationship between electrically conductive polymer and copper deposition,[32] adhesion between plated metal and 3D-printed polymer,[37] mechanical properties of copper-plated 3D-printed structures.[38]

Despite all the benefits of electroplating and electroless process in reducing electrical resistance by plating the 3D-printed electrically conductive polymer with copper, there is a major drawback characterizing these metallization techniques: only external features can be plated. At the state of the art, internal conductive features, completely embedded within 3D-printed dielectric parts are virtually impossible to be plated with metal. This huge limitation does not allow us to take full advantage of MEX technology, as the fabrication of structures with embedded sensors (plated with metals) would level up the role of AM for the fabrication of electronic components.

In the present research paper, the authors present a novel method to overcome this issue, by directly plating with copper conductive tracks completely embedded within dielectric structures, manufactured via MEX. Electroplating is performed inside closed channels (accommodating 3D-printed electrically conductive tracks), without dipping the part inside the electrolyte bath: a great reduction in electrical resistance of 5 orders of magnitude is achieved. The authors demonstrated that the proposed approach can also be implemented on-board commercial MEX machines, by pausing the print, plating the 3D-printed sensor (electrically conductive polymer) with copper, and finally resuming the print to extrude dielectric polymer on top of the copper-plated sensor, in order to manufacture smart structures with embedded copper sensors with improved performance (sensitivity, resolution, and stability) compared to 3D-printed counterparts. Finally, the proposed electroplating approach was performed to 3D features (i.e., coils), completely embedded within polymeric structures: the applicability of the proposed method is not limited to planar tracks but also virtually extended to any 3D feature embedded inside dielectric polymers.

2. Experimental Section

2.1. Electroplating Inside Channels: Principle, Design and Additive Manufacturing

The main novelty underlying the present research was based on performing electroplating on internal electrically conductive layers completely embedded inside dielectric parts manufactured via MEX. At the state of the art, only external layers could be plated with copper by recurring electroplating or electroless plating techniques.[31–33] The proposed approach aimed at unlocking a new exciting scenario for MEX AM: the possibility of obtaining copper parts inside dielectric components by only processing polymers.

Having copper tracks, instead of electrically conductive polymer was vital to level up the role of MEX (and AM) for the fabrication of sensors, actuators, and circuits: higher conductivity (≈4 orders of magnitude), improved electrical properties, reduction of power loss due to the Joule effects, and improved thermal conductivity are some of the advantages of copper over electrically conductive polymers. The workflow of the present research is depicted in **Figure 1**.

The proposed approach was implemented by designing closed dielectric structures with internal fluidic channels equipped with a conductive track composed of electrically conductive polymer (1.5 mm thick) embedded at the bottom of the channel (see

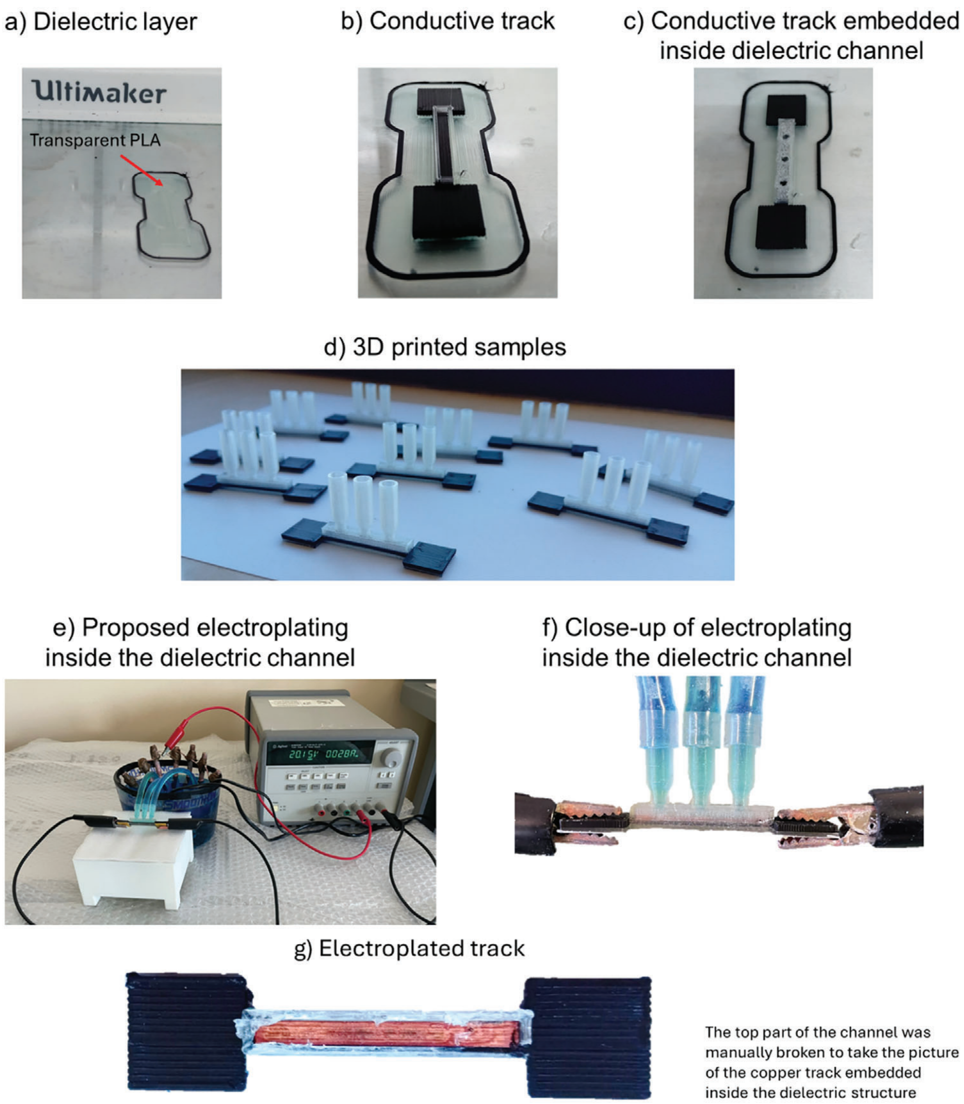

Figure 1. Workflow of the research: a) 3D printing of the base dielectric layer (PLA), b) 3D printing of the conductive track (CPLA) on top of the dielectric layer, c) 3D printing of the dielectric part in order to embed the conductive track inside the channel, d) final 3D-printed multi-materials samples to be electroplated, e) experimental setup to perform electroplating inside channels, f) close up view of the sample during the proposed electroplating process inside the closed channel, and g) electroplated track.

Figure 2a). The fluidic channel accommodated the electrolytic solution (used to perform electroplating) had a squared section of 3 mm × 4 mm, while the electrically conductive track to be plated with copper was initially designed 30 mm long, and afterward increased up to 100 mm to explore the capabilities and limitations of the proposed approach (see Section 3.2). It should be noted that the dielectric structure was equipped with three embedded connectors (two inlets, and one outlet) which would be connected to plastic tubes to perform electroplating outside the tank containing the electrolyte fluid (see Figure 2b). The reason underlying the usage of two inlets, instead of one, is detailed in Section 2.2.

A commercial dual extruder 3D printer (Ultimaker S5, Ultimaker, The Netherlands) was used throughout the whole research, to fabricate multi-material structures with no assembly steps. As dielectric material, a commercial polylactic acid (PLA) was used (PLA, Ultimaker, The Netherlands); while the electrically conductive polymer used to fabricate conductive tracks to be plated with copper was a conductive polylactic acid (CPLA) provided by Protopasta, USA. CPLA was characterized by a resistivity along the x-y plane and z-plane of 30, and 110 Ω · cm (Protopasta technical data sheet). The most important process parameters set for both materials in the slicing software (Ultimaker Cura 4.11) are listed in **Table** 1; it should be noted that process parameters used for CPLA had been selected with a trial-and-error approach and according to previous research work.[39]

Moreover, the CPLA track was composed of 7 adjacent 3D-printed lines (each extruded line is 0.4 mm width), and an infill line with a 90° orientation (aligned in the direction of the greatest dimension of the track, i.e., 30 mm) was set.

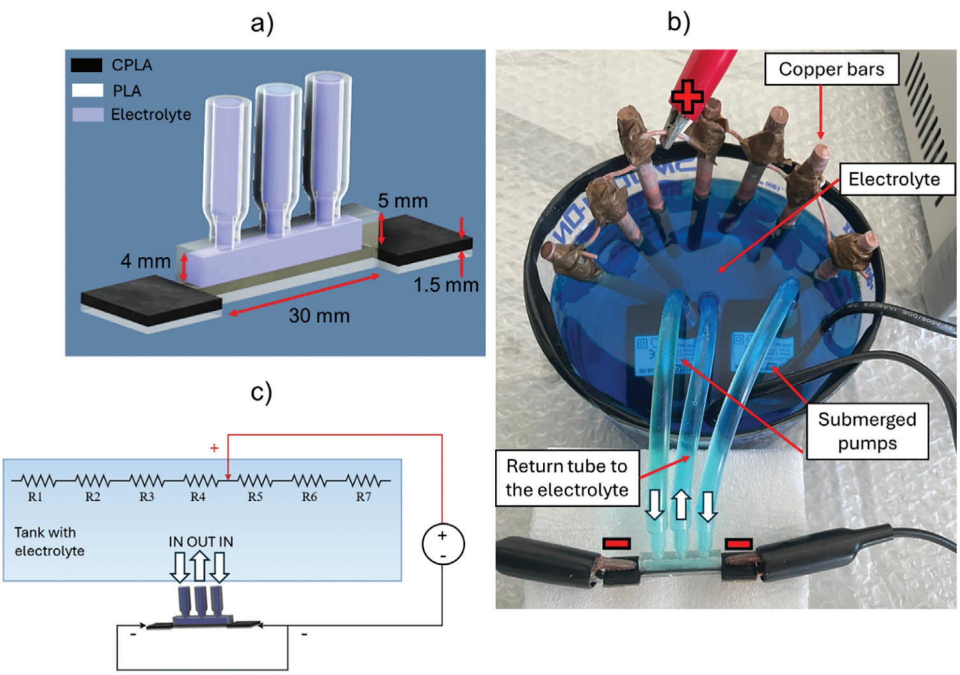

Figure 2. Proposed electroplating: a) multimaterial sample composed of transparent PLA, CPLA, and electrolyte fluid inside channels, b) electroplating setup including copper bars, electrolyte, electrical connections, submerged pumps, tubes, and 3D-printed sample, and c) electrical scheme of the proposed electroplating.

2.2. Electroplating Setup

The custom-made setup shown in Figure 2b) was used to perform electroplating inside channels. Differently from the state of the art,[31–33] in the proposed approach the electroplating technique was not performed by placing the 3D-printed sample inside the tank containing the electrolyte. The 3D-printed sample was located outside the tank, and it was connected to the electrolyte by means of plastic tubes and pumps which created the electrical circuit enabling the copper ions to transfer from the anode (copper bars) to the cathode (CPLA track) when electrical current was provided by the power supply. Such configuration unlocked the possibility to perform electroplating even on-board 3D printing machines during the fabrication of smart structures, by pausing the print and resuming it after the electroplating, as demonstrated in Section 3.3.

The proposed setup included a cylindrical tank filled up with electrolytes: a commercial electrolyte (TIFOO, Germany) was employed. Inside the tank, a total of 7 pure copper bars (99.9% copper) were arranged in a circular configuration and connected by means of pure copper wire (99.9%), acting as anode. In particular, 7 copper bars (trial-and-error approach) were found to be adequate to cover the whole cylindrical semi-perimeter of the tank: in this way, a consistent presence of copper ions was then provided near the return tube inside the electrolyte.

Two commercial inexpensive pumps, submerged inside the tank, were used to inject the electrolyte fluid inside the 3D-printed sample (through the embedded PLA connectors, in turns connected via plastic tubes to the pump) at 3.3 L/min for a total of 5 s. After that, the internal channel of the sample was completely filled up with electrolytes and the pumps were turned off. The pumps had a passive role (the electroplating was performed with the pumps off), as they were only needed to fill up both the internal channel and the returning tube, crucial to making copper ions move from the anode to the cathode. More details about the usage of the pumps in a passive way, instead of active, alongside CFD simulations, are provided in (Section S1, Supporting Information). As the authors envisioned this process to be largely used at several levels (from hobbyist to university research, to industrial), cost-effectiveness and widespread availability were of utmost importance for the pump selection. Common electric submersible pumps (Mingke, Submersible Pump 200 L h^{-1}) costing ≈8 euros each, often used for aquariums and fountains, were chosen. Such pumps (as many of the inexpensive pumps available on the market) have a fixed flow rate of 3.3 L min^{-1} which is too low

Table 1. Process parameters are set throughout the whole research.

Process Parameter	CPLA [Black]	PLA [Transparent]
Extrusion Temperature (°C)	240	210
Printing speed (mm s^{-1})	25	50
Layer thickness (mm)	0.2	0.2
External perimeters	0	2
Infill type	Lines 90 °	Lines 90 °
Infill density (%)	100	100
Flow (%)	110	100
Nozzle size (mm)	0.4	0.4
Line width (mm)	0.4	0.4
Fan (%)	0	50

Table 2. A factorial plan is performed to evaluate the best value of every parameter.

	Factors	
Levels	Current Density (A/dm^2)	Time (min)
Low (−1)	1	10
Middle (0)	3	30
High (+1)	5	50

to fill up the returning tube. This issue led the authors to use a two-inlet configuration (instead of one inlet), as the pressure produced by two pumps was enough to fill up the returning tube correctly.

The proposed electroplating setup worked according to the traditional two-electrodes system: the copper bars represented the anode, while the 3D-printed track (CPLA track) embedded inside the dielectric channel represented the cathode. Both the electrodes were connected to a DC power supply (Agilent E3631A), providing constant current to the circuit to make the copper electrodeposition happen. The electrical circuit representation of the proposed electroplating process is shown in Figure 2c).

2.3. Electroplating Parameters Investigation

Since the electroplating process inside closed channels to the plate with copper 3D-printed tracks was hereby presented for the first time, an extensive study about the main electroplating parameters affecting the final electroplated track was carried out. To assess the best electroplating process parameters, two main factors were investigated: current density (A/dm^2), and electroplating time (min). For each factor, three levels were studied, namely low (−1), middle (0), and high (+1) levels. All the values associated with every level, for every factor, are listed in **Table 2**. A full factorial plan, with a total of 9 combinations and three replications, was performed. The minimization of electrical resistance (Ω) measured after performing electroplating was the response variable of the factorial plan. Scientific literature was analyzed to define the values of each level, according to the ones generally employed for traditional electroplating techniques on 3D-printed parts. Samples having the dimensions shown in Figure 2a) had been fabricated, for a total of 27 samples. In particular, the CPLA track was arbitrarily designed 30 mm long, 1.5 mm thick, and 2.8 mm wide (smaller and longer tracks can be electroplated, as demonstrated in Section 3.2). A benchtop multimeter (GW Instek GDM-8341) was employed to measure electrical resistance, before and after electroplating. The mean electrical resistance measured on every sample after the 3D printing process (before performing electroplating) was equal to 2300 Ω ± 63Ω. After performing electroplating, the top part of the sample (channel enclosure with pump connectors) was manually opened (removed by breaking it with a cutter) to take pictures of electroplated copper inside the channel otherwise impossible to be seen. Also, a digital microscope (Tomlov TM-DM11, Tomlov, USA) was used to take pictures of the plated tracks to evaluate the uniformity of the copper deposition as a function of different combinations.

3. Results

3.1. Electroplating Parameters to Minimize Electrical Resistance

As described in Section 2.3, two main electroplating parameters (current density, and time) have been correlated to the electrical resistance obtained after performing electroplating. The mean electrical resistance value measured for every combination, after performing electroplating, is shown in **Table 3**.

From the electroplating process parameters investigation (which results are consistent, as shown in the Section S2, Supporting Information), the following conclusions can be drawn:

Current density and electroplating time produce an effect on the minimizing of the resistance: for both of them, when switching from low level (−1) to high level (+1) a remarkable reduction in resistance is achieved, as shown in **Figure 3a**). On the other hand, the combination of both parameters does not produce any effect.

A current density of 5 A/dm^2 and time of 50 min were found to be the best parameter combination to minimize electrical resistance: a final resistance of 0.08 Ω was obtained. It should be noted that similar results were also obtained when i) the current density was reduced to 3 A/dm^2 and the time was either 30 min and 50 min (respectively, 0.12, and 0.1 Ω), and ii) the current density was 5 A/dm^{2}and the time was shortened to 30 min (0.1 Ω), as demonstrated by the voltage drop over the circuit (See Section S3, Supporting Information). Such results suggest that the minimum current density and electroplating time to obtain a consistent copper deposition, thereby resulting in a resistance lower than 1 Ω are 3 A/dm^2, and 30 min. Figure 3b) shows the effect of the current density and electroplating time on the final electrical resistance.

Pictures taken by means of a digital microscope are in good agreement with the electrical resistance values measured after the electroplating process. As shown in Figure 3c), when setting the parameters (1 A/dm^2, and 30 min) resulting in the lowest electrical resistance reduction (630 Ω), an inconsistent copper deposition was observed. Only a small surface was plated with copper thereby resulting in a higher electrical resistance. When both the electroplating time and current density were increased, a higher amount of copper was observed on top of the

Table 3. Mean electrical resistance after performing electroplating inside the channel for every combination.

Combination	Current Density [A/dm^2]	Time [min]	Mean electrical Resistance [Ω]
(a)	1	10	980
(b)	3	10	630
(c)	5	10	500
(d)	1	30	900
(e)	3	30	0.12
(f)	5	30	0.1
(g)	1	50	650
(h)	3	50	0.1
(i)	5	50	0.08

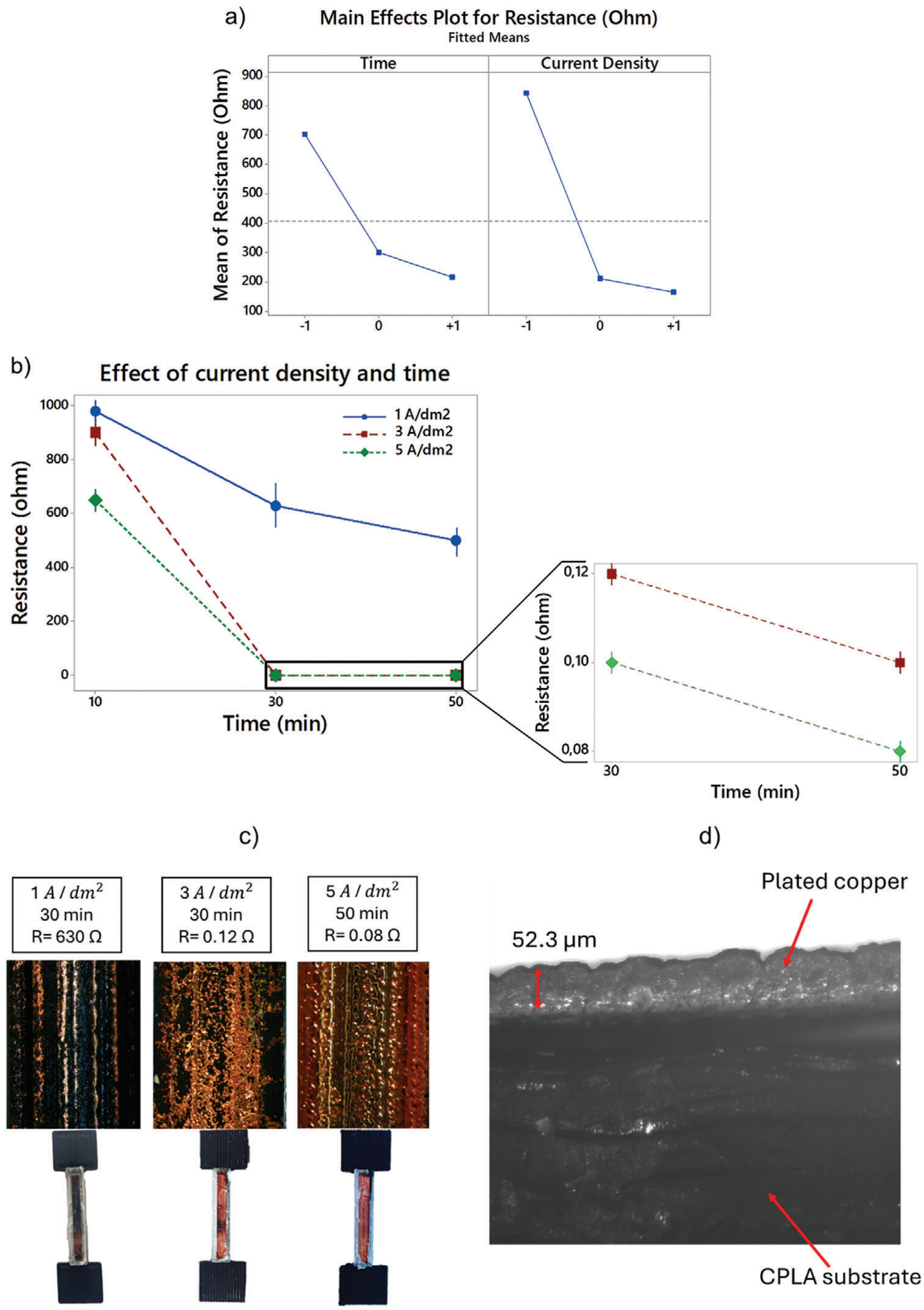

Figure 3. a) Main effect of the two parameters investigated, b) Effect of current density and time, c) copper deposition as a function of the electroplating parameters, and d) plated copper thickness (5A, 50 min).

electrically conductive polymer. The parameters resulting in the lowest electrical resistance produce a very consistent copper distribution covering the whole surface of the 3D-printed CPLA track.

In conclusion, the results obtained from the factorial plan highlight the correlation between electroplating parameters and resistance reduction: in particular, the higher electrical resistance reduction (0.08 Ω) is achieved when 5 A/dm^2 were provided for a time of 50 min. It should be noted that for every combination (repeated 3 times) a very low standard deviation was obtained, as depicted in Figure 3b), proving the consistency of the proposed electroplating approach.

Moreover, an optical microscope (Precise Eye fixed system, Navitar, USA) was used to evaluate the thickness of the plated copper under the optimal parameters. The thickness of the deposited copper was uniform among all the length (30 mm) of

Table 4. Reduction in resistance and actual current provided to obtain 5 A dm^{-2} for every track length.

Track Length	Current [A]	Resistance -as Printed [Ω]	Resistance – after Electroplating [Ω]
30	0.042	2300	0.08
40	0.056	2700	0.09
50	0.07	3200	0.11
100	0.14	4700 (as printed) 2500 (after performing ironing)	0.17

the electrically conductive track (see Section S4, Supporting Information), resulting in a mean thickness of 52.3 µm. Figure 3d) shows the thickness of the deposited copper in the middle of the sample. It should be noted that the thickness of the plated copper (52.3 µm) is in good agreement with the theoretical value (55.1 µm) of the deposited copper layer calculated according to Faraday's laws of electrolysis:

$$\delta = 10^4 \frac{M_w}{n\,F\,\rho\,A} \int idt \tag{1}$$

where δ (µm) represents the final thickness of the plated copper, M_w (g/mol) is the atomic weight of copper, n is the number of electrons taking part in the reduction reaction, F (C/mol) is the Faraday constant, ρ (g/cm^3) is the density of the copper, A (cm^2) is the area of copper deposition, i (A) is the current applied during the electroplating, t (s) is the electroplating time, and 10^4 is a scaling factor to convert cm to µm.

The neglectable discrepancy of 2.8 µm between the measured thickness value of 52.3 µm and the theoretical value of 55.1 µm calculated according to Equation (1), could be related to small current inefficiencies often characterizing electroplating processes.

3.2. Capabilities and Scalability

To fully characterize the proposed approach, a scalability test was performed to demonstrate that CPLA tracks inside dielectric channels can be scaled up, and down. The same geometry tested in Section 3.1 was scaled up: samples with an embedded CPLA track of 40, 50, and 100 cm were fabricated. The same process parameters were found to minimize the electrical resistance, namely the current density of 5 A/dm^2 and a time of 50 min, was set for the electroplating process. As depicted in **Figure 4a**), for all the samples a very good copper deposition was obtained, thereby resulting in a great electrical resistance reduction (see **Table 4**). More details about the plated copper uniformity for the longer track (100 mm) are provided in Section S5 (Supporting Information). As shown in Table 4, in order to provide a current density of 5 A/dm^2 different values of electrical current (A) have to be set for every sample (according to the length): in particular, for the 100 mm CPLA track, a current of 0.15 A was required. The longer the CPLA track, the higher the electrical current value to be set to provide 5 A/dm^2. Such correlation might result in heating issues: high values of current might overheat the sample (Joule effect), thereby resulting in structural damages (i.e., deflection) and safety problems. This problem needs to be considered when very long tracks have to be electroplated. Equation (1) expresses the direct correlation between current and heat:

$$\frac{dQ}{dt} = i^2 R - \dot{Q}_{cond} - \dot{Q}_{conv} - \dot{Q}_{rad} \tag{2}$$

where $\frac{dQ}{dt}$ (W) represents the total rate of heat accumulated during the electroplating, $i^2 R$ (W) is the heat generated through the Jouel effect, $\dot{Q}_{cond}$ (W), $\dot{Q}_{conv}$ (W), and $\dot{Q}_{rad}$(W) represents the rate of heat loss due to conduction, convection, and irradiation, respectively.

A simple, cost-effective, and efficient way to reduce electrical resistance in 3D-printed conductive tracks consists in performing ironing during the 3D printing process. As demonstrated in,[39] the ironing parameter which repeats the last extruded layer by passing the hot nozzle over it (without extruding any material), greatly reduces electrical resistance. Such a technique was used by the authors, to reduce the term R of Equation (2) for the 100 mm long CPLA track from 4700 to 2400 Ω: in this way, overheating problems were avoided, and the Joule effect was mitigated. As a matter of fact, a thermal camera was used to monitor the temperature throughout the electroplating process and a constant temperature of 28 °C was recorded.

To further prove the potentialities of the proposed approach, small-scale and non-straight CPLA tracks have been electroplated: in particular, zig-zag (2.2 mm long), and circular (1.8 mm long) CPLA tracks were 3D-printed inside channels as shown in Figure 4b,c and subsequently electroplated (by setting the optimal electroplating parameters). A remarkable reduction of electrical resistance for both structures was obtained (zig-zag equal to 0.06 Ω, and circular equal to 0.05 Ω), demonstrating that the proposed approach can be successfully used to plate with copper small-scale non-straight conductive tracks.

The proposed approach requires an additional amount of polymeric material (PLA) for fabricating the fluidic ports (inlets and outlets), which remain permanently anchored to the structure unless manually removed. According to the slicing software (Ultimaker Cura 4.11), this extra material usage is minimal, amounting to just 4 g per fluidic port. For future developments, the authors envision utilizing filament-based MEX machines capable of processing more than two materials simultaneously.[1] This would enable the use of a sacrificial, water-soluble material (e.g., polyvinyl alcohol) for the fluidic ports, electrically conductive materials for the tracks, and any polymer for the external structure. This approach offers a significant advantage: after completing the proposed electroplating, the fluidic ports can be directly dissolved by immersing the final structure in water for a few minutes.

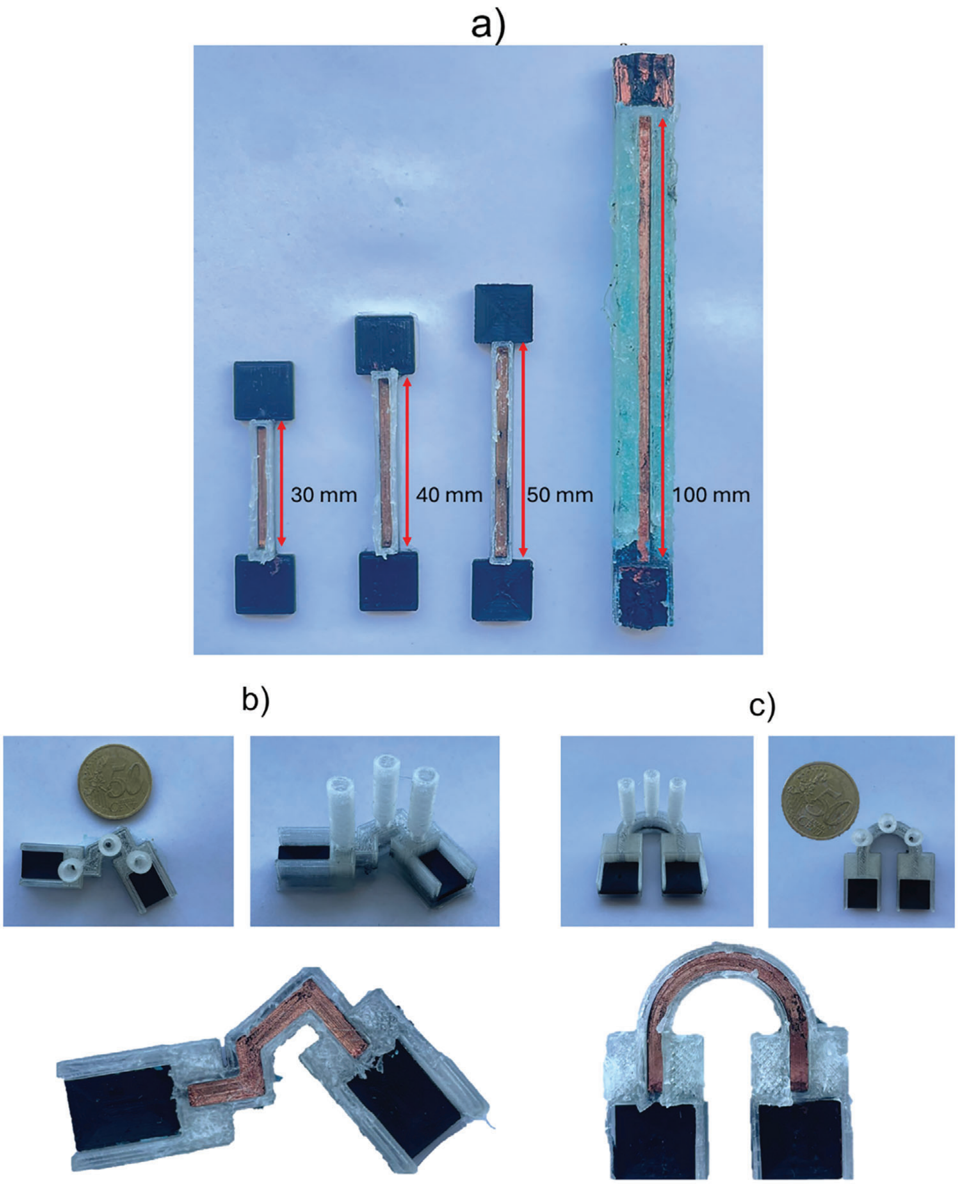

Figure 4. Scalability of the proposed electroplated approach: a) electroplating performed on different lengths (from 30 mm up to 100 mm), b) electroplating performed on zig-zag small-scale structure, and c) electroplating performed on the circular small-scale structure.

3.3. On Board Electroplating for Embedded Copper Planar Sensors

In this section, the authors describe a robust methodology to perform the proposed electroplating approach directly on board commercial MEX machines, to fabricate smart structures with embedded copper sensors (instead of electrically conductive polymers) with no assembly tasks, employable to self-detect force inputs. The workflow underlying the proposed methodology to perform electroplating on board a commercial MEX 3D printer is here described, and depicted in **Figure 5**:

1) First, the dielectric PLA base was extruded by means of extruder 1, and subsequentially extruder 2 was used to fabricate the CPLA sensor on top of the PLA base (Figure 5a). The CPLA sensor is composed of 5 extruded layers, for a total thickness of 1 mm (layer thickness of 0.2 mm).
2) After extruding the last CPLA sensor layer, the print is automatically paused: an extension was added to the slicing software (Ultimaker Cura 4.11) to pause the print after extruding the desired layer. It should be noted that during the pause, i) the printhead was parked in the left corner of the machine, and ii) the build plate was lifted down. Both these actions were needed to avoid collisions and increase the working space while performing electroplating
3) A custom-made PLA coverage composed of three pump connectors (two inlets, and one outlet) connected to an internal fluidic channel that reproduces the negative geometry of

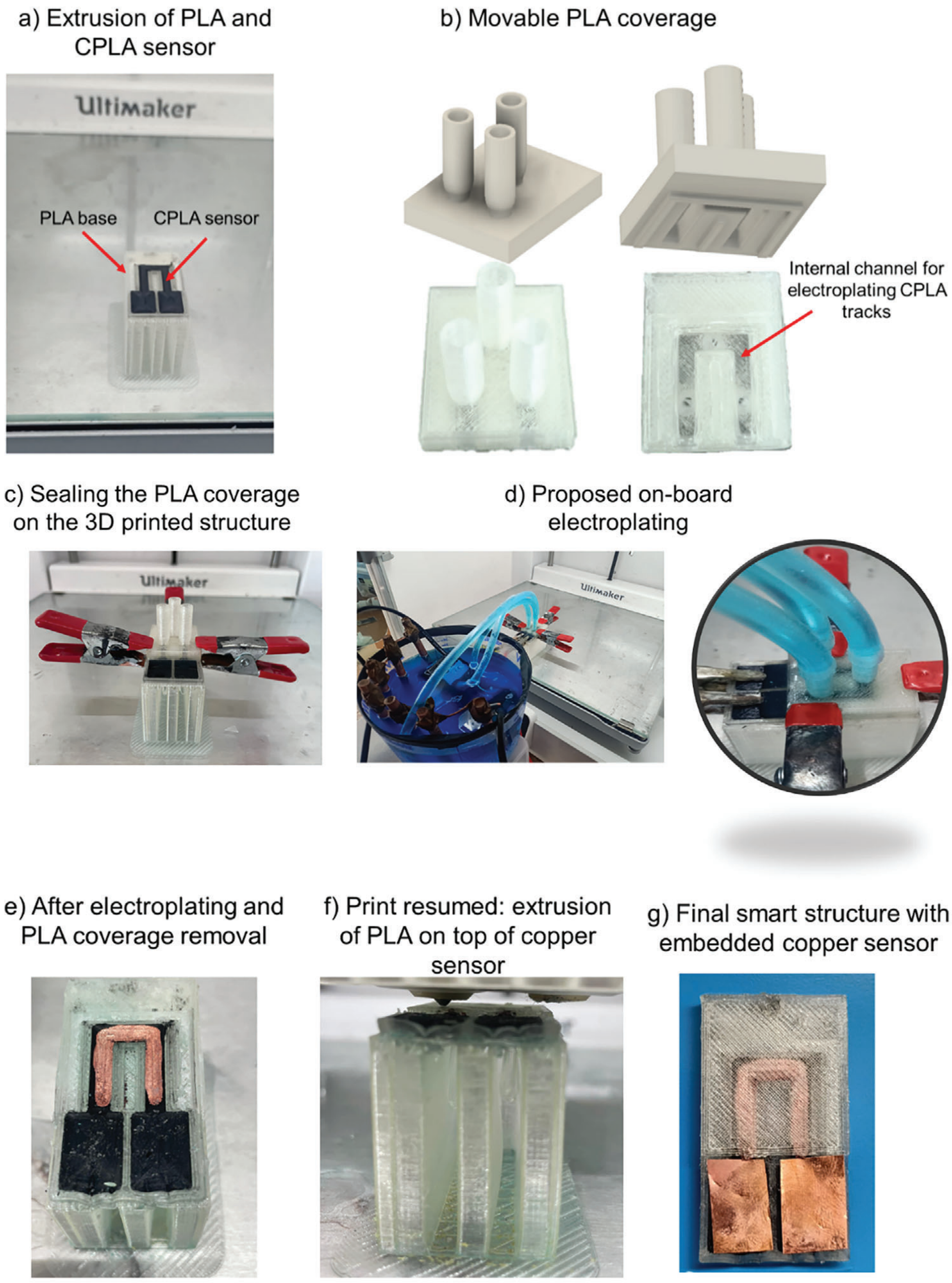

Figure 5. On-board electroplating: a) After extruding the PLA base and CPLA sensor, the print was automatically paused b) Movable PLA coverage with internal channel to be placed on top of the 3D-printed structure to perform electroplating, c) Sealing the movable PLA coverage on top of the 3D-printed structure, d) performing the proposed on-board electroplating, e) CPLA covered with copper after performing electroplating: it should be noted that the movable PLA coverage was removed, f) Resuming the print and extruding PLA on top of the copper, g) Final smart structure with embedded copper sensor, it should be noted that thin copper layers were glued on the pads in order to solder electrical wires.

the CPLA sensor was employed (see Figure 5b). Such PLA coverage is a movable element that is manually attached to the 3D-printed part (when the print is paused), and subsequently removed (when the electroplating process is completed) allowing the print to be resumed to extrude PLA on top of the just plated copper, to fully embed the sensor. The PLA coverage was assembled on top of the 3D-printed structure by recurring to steel spring clams, used to apply pressure between the PLA coverage and the 3D-printed structure (in conjunction with silicone rings placed between the CPLA sensor and the top coverage) to guarantee electrolyte tightness during the whole electroplating process (Figure 5c).

4) After sealing the PLA coverage, the electroplating setup (including electrolyte bath, pumps, and power supply) was connected to the 3D-printed structure (as described in

Section 2.2), and a current density of 5 A/dm^2 for 50 min (best parameters found in Section 3.1) was provided (Figure 5d).

5) After 50 min, the electroplating process was stopped, and the PLA coverage was manually removed (Figure 5e): the CPLA sensor results to be completely plated with copper.
6) The print is resumed, and dielectric PLA is extruded on top of the copper tracks, to fully embed the copper sensor inside the dielectric structure (Figure 5f). After extruding three PLA layers, the final smart structure with embedded copper sensor is ready to be removed from the build plate. Particular attention was paid to the electrical contacts: after the fabrication, a thin copper film (same dimension as the pad) was glued on top of the pads to create electrical continuity with the copper tracks (Figure 5g). Afterward, electrical wires were soldered on top of every copper pad.

The smart structure fabricated by means of the proposed approach (**Figure 6**a) is 25 mm wide, 45 mm long, and 3 mm thick, including a sensor track which is 2.8 mm wide, and 15.5 mm long. Also, three layers of PLA have been extruded on top of the electroplated sensor, resulting in an overall thickness of 0.6 mm covering the copper tracks. The same process parameters listed in Table 1 have been used. The printing time estimated by the slicing software was 48 min, the electroplating process took 50 min, a total of ≈10 min was required to connect the 3D-printed part to the electroplating setup and seal the PLA movable coverage, and 5 min was required to disconnect the 3D-printed part from the electroplating setup, thereby resulting in a total of 113 min to fabricate a PLA smart structure with embedded copper sensor.

As shown in Figure 6b, when recurring to the proposed on-board electroplating, a great electrical resistance reduction is obtained: a final resistance of 0.09 Ω was obtained, against 2375 Ω charactering the traditional CPLA sensor. It is worth noting that both 2-point and 4-point electrical resistance measurements were performed, yielding the same value of 0.09 Ω. This result indicates that the contact points have no impact on the measurement.

Both the proposed copper-based smart structure and traditional CPLA-based have been tested to fully characterize all the benefits related to the proposed on-board electroplating methodology in terms of sensor performance: several tests were carried out, and hereby discussed.

A universal testing machine (INSTRON 34TM10) was used to apply force on top of the sensor by moving the traverse (a tool applying force was attached to the traverse) down at a rate of 1 mm min^{-1}. The test was stopped when a force value of 10 N was reached. The applied force was measured from the testing machine (by means of a load cell with a resolution of 0.01 N), and the change in electrical resistance of the sensor was measured by means of a benchtop multimeter connected to the laptop to collect data. Figure 6c shows the custom-made setup. It should be noted that a force perpendicular to the direction of the greatest dimension (length of 45 mm) of the 3D-printed structure was applied, resulting in the bending of the 3D-printed smart device. The proposed strain sensor operates based on the piezoresistive effect: electrical resistance changes in response to applied mechanical stress (such as bending) which deforms the material structure and alters electron flow pathways.

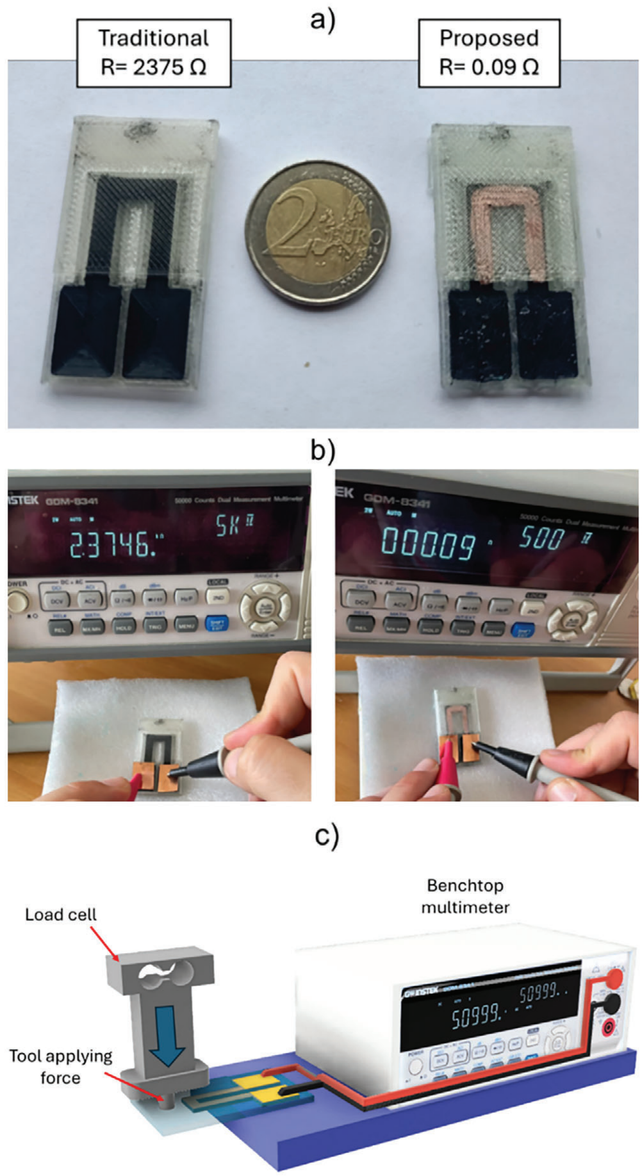

Figure 6. a) proposed copper smart structure and its traditional counterpart, b) electrical resistance reduction, and c) setup employed to characterize the proposed and traditional smart structure.

Electrical resistance was normalized ($\Delta R/R_0$), and plotted against force, as depicted in **Figure 7**a). The same test was carried out for both the proposed smart structure (copper sensor), and the traditional one (CPLA sensor) for a total of three time, to consider variability as well. As shown in Figure 7a), the proposed smart structure with embedded copper sensor is characterized by a higher sensitivity compared to the traditional CPLA-based structure: a greater change in normalized resistance ($\Delta R/R_0$) is obtained when the same force input is applied. As a matter of fact, the proposed sensor is characterized by a sensitivity (1/N) of 0.06, against 0.0017 of the traditional sensor. Another remarkable benefit related to the proposed copper-based smart structure is the higher resolution of 0.05 N (minimum force detectable from the sensor), against 3 N characterizing the

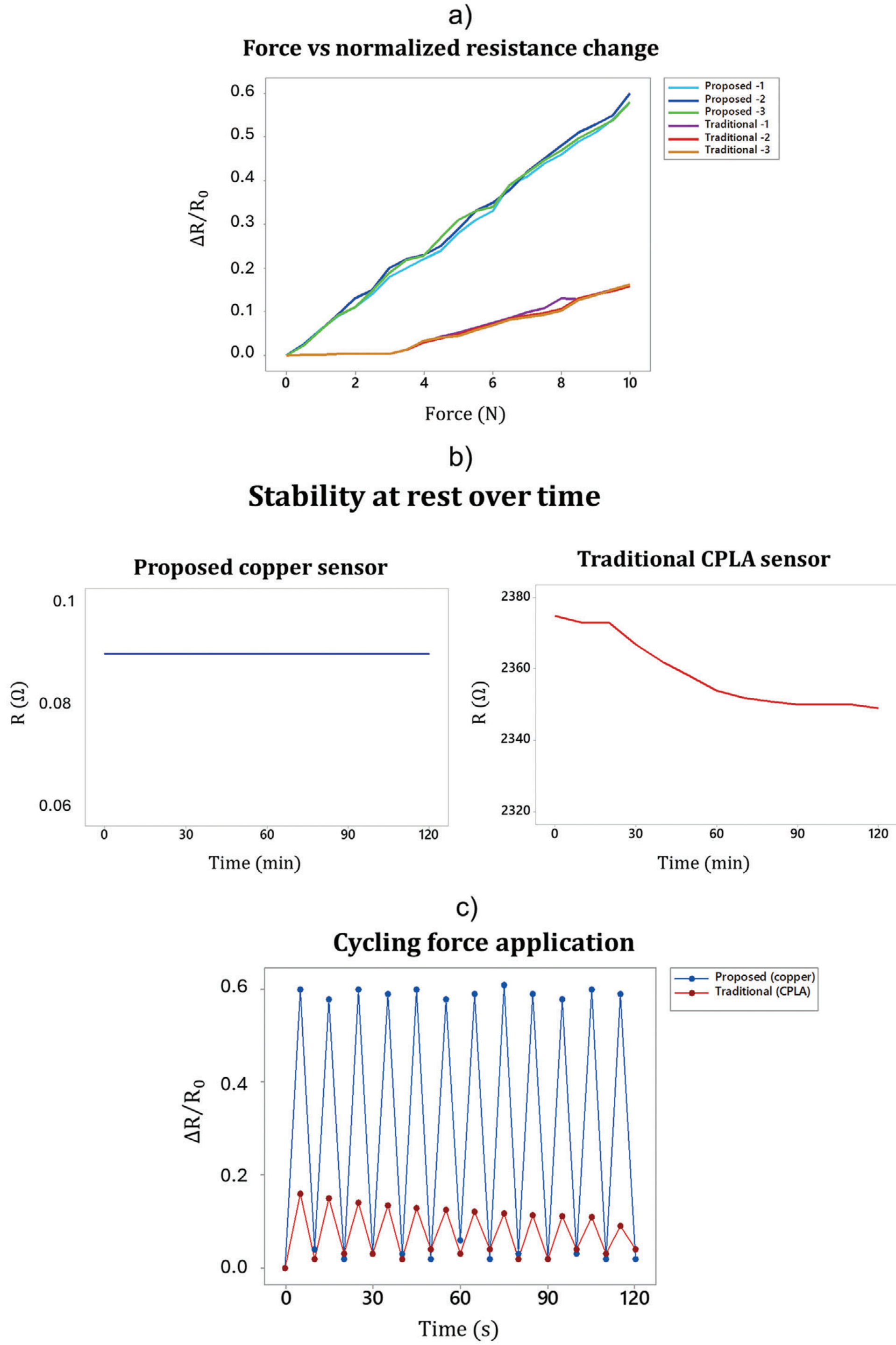

Figure 7. Characterization of the proposed smart structure with copper sensor and comparison with traditional 3D-printed smart structure: a) force versus change of normalized resistance, b) stability at rest, and c) stability when a force of 10 N is cyclically applied at 0.2 Hz.

traditional CPLA-based structure. These results (improved sensitivity, and higher resolution) are strongly related to the chemical composition, atomic structure, and physical conductive mechanisms which differ from copper (free electrons moving inside an ordered crystalline structure) to electrically conductive polymer (disordered polymer chain with random networks of conductive fillers according to the percolation theory).[40] A common issue, negatively affecting electrically conductive polymers–based 3D-printed sensors is the high instability of the sensor readings, even when no force is applied.[39,41] Such a phenomenon was considered, and both the proposed and traditional sensors were connected to the benchtop multimeter for a total of 2 h each,

Table 5. Summary of the performance of the proposed copper-based smart structure benchmarked with traditional CPLA-based smart structure.

	Resistance	Sensitivity [1/N]	Resolution	Stability [at rest]	Stability [100 N at 0.2 Hz]
Proposed (embedded copper sensor)	0.09 Ω	0.06	0.05 N	Stable	Stable
Traditional (embedded CPLA sensor)	2375 Ω	0.0017	3 N	Not stable: decreasing drift of – 0.025 Ω/min	Not stable: decreasing drift of – 0.28 Ω/min

without applying any force (rest condition), to record resistance values over time. As depicted in Figure 7b), the proposed sensor shows great stability: the same resistance value of 0.09 Ω was recorded throughout the whole 2 h test. On the other hand, the traditional CPLA-based smart structure is characterized by a decreasing drift in the sensor response. At the beginning of the test an electrical resistance equal to 2375 Ω was recorded, while at the end of the test a resistance of 2348 Ω was obtained. A linear regression model was used to fit the data, and calculate the slope of the decreasing curve, to evaluate the instability of the sensor. A slope equal to–0.025 Ω/min was obtained ($R^2 = 0.89$), indicating a great resistance drift, when no force is applied. Also in this case, the proposed copper-based smart structure exhibits higher performance compared to its counterpart, as there was no drift in the sensor response while it was tested at rest.

A final test to evaluate a possible drift while applying force was performed: a force of 10 N was applied at a frequency of 0.2 Hz, for a total time of 120 s. Also in this case, the proposed copper-based sensor does not exhibit any drift trend, while the traditional CPLA sensor was characterized by a decreasing trend of–0.28 Ω/min ($R^2 = 0.94$), as shown in Figure 7c.

The reason underlying the decreasing drift in the traditional CPLA-based sensor (and in general, in electrically conductive polymer- based 3D-printed sensors) is not fully understood in scientific literature; however, a possible explanation concerns the change in temperature inside electrically conductive polymer (CPLA) due to the interaction between the current flowing inside the CPLA and the high electrical resistance of the CPLA sensor (Joule effect). As the electrical resistance of the proposed copper-based sensor is reduced (5 orders of magnitude smaller), the Joule effect is mitigated, and no decreasing drifts occur neither at rest nor when cyclically applying force.

In conclusion, the proposed on-board electroplating approach allows the direct additive manufacturing of smart structures with embedded copper sensors, without recurring to any assembly task. The copper-based smart structure, is characterized by im-

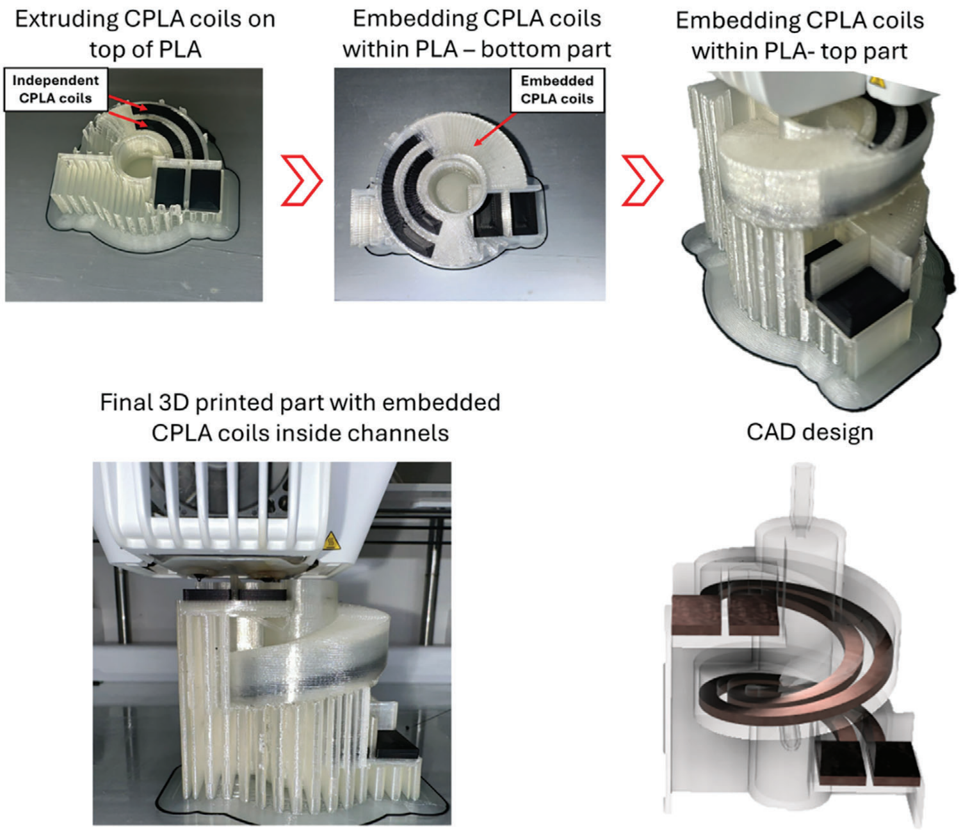

Figure 8. Fabrication of the spiral-shaped structure with embedded independent CPLA coils.

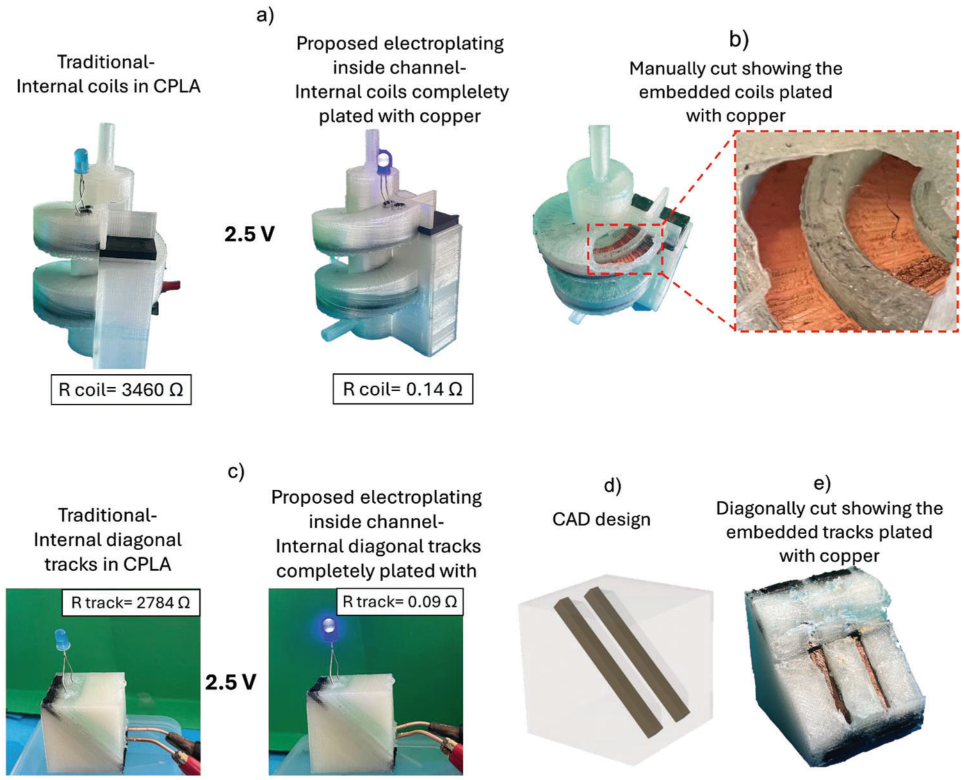

Figure 9. Proposed electroplating performed on the spiral-shaped structure, and cubical structure: a) comparison between electroplated structure (coils plated with copper inside channels) and traditional structure (CPLA coils) when applying 2.5 V with LED light, b) isometric view: it is possible to see the thin copper layer plated on top of the CPLA coils, as the closed structure was manually cut to take the picture.

proved performance compared to its counterpart (smart structure with embedded electrically conductive polymers), in particular a sensitivity (1/N) of 0.06 with a minimum resolution of 0.05 N is achieved against a sensitivity (1/N) of one order of magnitude lower (0.0017) and a lower resolution of 3 N. Also, the proposed copper-based structure is characterized by a great stability in the sensor response, both at rest and when cyclically stressed, due to a reduced electrical resistance which mitigates overheating phenomenon related to the Joule effect. In addition, the proposed electroplated copper sensor demonstrated a Gauge Factor (GF) of 2.7(ratio between change in resistance and strain), which is comparable to traditional strain sensors fabricated using costly screen-printing and lithography techniques.[42] This value is also consistent with commercially available metal strain sensors, which typically exhibit a GF ranging from 2 to 5.

Table 5 summarizes the main results obtained from the proposed copper-based smart structure compared to the traditional CPLA-based counterpart.

3.4. Electroplating for 3D Geometries Embedded within Dielectric Structures

The present section aims at expanding the applicability of the present study from planar structures (i.e., strain gauge sensor shown in Section 3.3) to 3D features embedded within dielectric parts. Having complex 3D copper features completely embedded within plastic structures could be extremely beneficial for the fabrication of i) sensors with unconventional geometries to detect multiple variables, ii) functional electrical devices such as inductors,[31] and iii) complex internal copper circuits.[43] The latter has been extensively studied: at the state of the art, the most viable solutions are represented by either pausing the print to manually embed copper elements or using external expensive systems (i.e., ultrasonic robotic tool).[44] The proposed approach applied to 3D structures (non-planar) could potentially bring the following advantages: i) cost-effectiveness (as no expensive tools are required to embed copper elements), and ii) zeroing assembly tasks (as complex structures can be monolithically manufactured).

Two demonstrations are provided in the present section: a spring-shaped structure with embedded coils, and a cubical structure with embedded diagonal tracks.

The fabrication process of the spring-shaped structures with two embedded independent CPLA coils is shown in **Figure 8** The proposed structure is equipped with two independent CPLA coils (they do not touch each other), having a thickness of 3 mm, width of 5 mm, and spaced by 3 mm of dielectric PLA. The CPLA coils are embedded within a channel having the same thickness of the channel shown in Figure 2a). The total height of the spring-shaped structure is 80 mm, resulting in a total loop length of both coils of 471 mm, an outer diameter of the coils of 32, and 48 mm (respectively for the internal and external coil), and a total of two revolutions per coil. A total of 3 h and 42 min was required to fabricate the whole structure. The same process parameters listed in Table 1 were used. After the 3D printing process, the electrical resistance was measured and a value of 3460 Ω was recorded. The proposed electroplating process was performed, for a total of 100 min (50 min per coil).

After performing electroplating, the resistance was lowered from 3460 to 0.14 Ω for both the coils, thereby proving that the proposed electroplating inside channels works well also for complex 3D structures. The repeatability of the proposed approach was also evaluated by fabricating and electroplating a total of 5 spring-shaped structures: a mean electrical resistance of 0.15 Ω, with an extremely low standard deviation of 0.01 Ω was achieved. This demonstrates that the proposed electroplating technique within closed channels is highly repeatable and effective, even for intricate 3D geometries. Future works will focus on the usage of X-ray Computed Tomography, a technique proven to efficiently detect micro-features (i.e., voids) in 3D-printed parts)[45,46] to analyze the uniformity and thickness of thin layers of copper in complex 3D geometries electroplated using the proposed approach.

A blue LED light was connected on the top part of the coils (through two holes), and a voltage of 2.5 V was provided through the bottom pads. Due to the extremely low resistance of both coils, the LED light was immediately turned on, for the electroplated structure. The same test was performed for the counterpart spring structure having CPLA coils (no electroplated was performed), and as expected the LED light was not turned on, due to the extremely high resistance of the CPLA coils (3460 Ω for every coil). **Figure** 9a depicts such behavior. As the plated coils are completely embedded within dielectric PLA, the copper deposition cannot be immediately appreciated without removing the dielectric PLA. For this reason, the authors manually cut (destructive test) the top part of the spring to take pictures of the thin layer of copper on top of the CPLA coils: Figure 9b shows a part of plated coils in the 3D space. The second demonstrator is represented by a cubical structure (smart dice inspired by),[47] having two independent internal diagonal CPLA tracks running through the whole height of the cubical structure. The 3D diagonal tracks have a width of 3 mm, thickness of 3, and length of 40 mm (equal to the height of the cube) and separated by 11 mm of dielectric PLA. After the fabrication, the proposed electroplating process was performed, and the resistance was lowered from 2784 to 0.09 Ω (almost the same reduction obtained in 3.1 for planar tracks). The LED light test was performed: only the LED light connected to the plated tracks was turned on when a voltage of 2.5 V was supplied (See Figure 9c). As for the spiral-shaped structure, the plated tracks are completely embedded within the cube, thereby making it impossible to be seen. For this reason, a diagonal cut was performed: the embedded independent diagonal tracks completely plated with copper are shown in Figure 9e.

4. Conclusion

In the present research paper, a novel methodology to plate with copper internal features manufactured by means of AM MEX is presented. At the state of the art, only 3D-printed external features can be electroplated: the proposed approach unlocks the possibility of obtaining copper features embedded inside dielectric structures, with no assembly tasks, to fully exploit AM and fabricate self-sensing structures with improved performance. Current density, electroplating time, and electrolyte flow were investigated, and the optimal configuration (5 A/dm^2, 50 min, and 0 L/min) was proven to abruptly reduce the electrical resistance of 3D-printed electrically conductive tracks of 5 orders of magnitude (from 2300 to 0.08 Ω). The scalability of the proposed electroplating approach was also investigated, demonstrating that tracks 100 mm long can be plated with copper (only if the ironing strategy is performed), as well as small scale not-straight (circular, and zig-zag) tracks. A robust methodology to perform electroplating on-board commercial MEX machines is presented: after extruding electrically conductive polymer, the print is paused and the electroplating process is directly performed on board the 3D printer machine (by recurring to a movable structure with channels), afterward the print is resumed, and the dielectric material is extruded on top of the just electroplated copper to completely embed copper tracks inside the structure. The proposed copper-based smart structure was tested showing superior performance, in terms of resolution, stability, and sensitivity, compared to traditional 3D-printed smart structures. Finally, the proposed methodology was used to plate with copper 3D features completely embedded within dielectric structures (two independent coils embedded within a spiral-shaped structure, and two diagonal tracks within a cube), proving that embedded 3D copper circuits can be manufactured with easy by means of MEX.

The present paper aims at elevating the role of MEX for the fabrication of structures with electronics: as copper has superior performance compared to electrically conductive polymers, the proposed electroplating approach can be used to directly additive manufacture assembly-free complex structures, such as functional and smart devices, with internal copper features (planar and 3D).

Supporting Information

Supporting Information is available from the Wiley Online Library or from the author.

Acknowledgements

The following research work was supported by the following funding sources: BRIEF—Biorobotics Research and Innovation Engineering Facilities—Missione 4, "Istruzione e Ricerca"—Componente 2, "Dalla ricerca all'impresa"—Linea di investimento 3.1, "Fondo per la realizzazione di un sistema integrato di infrastrutture di ricerca e innovazione", funded by European Union—NextGenerationEU, CUP: J13C22000400007. National Recovery and Resilience Plan (NRRP), Mission 4 Component 2 Investment 1.3 – Call for tender No. 341 of 15/03/2022 of Italian Ministry of University and Research funded by the European Union – NextGenerationEU. Award Number: PE00000004, Concession Decree No. 1551 of 11/10/2022 adopted by the Italian Ministry of University and Research, CUP D93C22000920001, MICS (Made in Italy – Circular and Sustainable). Italian Ministry of University and Research under the Programme "Department of Excellence" Legge 232/2016 (Grant No. CUP – D93C23000100001) National Institutes of Health grant U12AB123456 (PV, CHO).

Open access publishing facilitated by Politecnico di Bari, as part of the Wiley - CRUI-CARE agreement.

Conflict of Interest

The authors declare no conflict of interest.

Author Contributions

A.P., G.S., M.D., and G.P. performed conceptualization. G.S., M.D., and G.P. performed methodology. M.D. performed the investigation. A.P., M.D., and G.S. performed visualization. G.P. funded acquisition. G.P. performed project administration. G.S. and G.P. performed supervision. G.S. and G.P. wrote the original draft. G.S. and G.P. wrote, reviewed, and edited the final manuscript.

Data Availability Statement

The data that support the findings of this study are available in the supplementary material of this article.

Keywords

3D printing of copper, 3D-printed sensors, electroplating, embedded sensors, material extrusion, smart structure

Received: November 15, 2024
Published online: December 10, 2024

[1] J. Cañada, H. Kim, L. F. Velásquez-García, *Virtual Phys. Prototyp.* **2024**, *19*, 2310046.
[2] P. F. Flowers, C. Reyes, S. Ye, M. J. Kim, B. J. Wiley, *Addit. Manuf.* **2017**, *18*, 156.
[3] N. Lazarus, H. H. Tsang, *IEEE Trans. Components, Packag. Manuf. Technol.* **2020**, *10*, 1965.
[4] J. D. Banks, A. Emami, *3D Print. Addit. Manuf.* **2022**, *11*, 2.
[5] S. Safaee, M. Schock, E. B. Joyee, Y. Pan, R. K. Chen, *Addit. Manuf.* **2021**, *51*, 102642.
[6] J. A. Hernandez, C. Maynard, D. Gonzalez, M. Viz, C. O'Brien, J. Garcia, B. Newell, T. N. Tallman, *Addit. Manuf.* **2022**, *58*, 102948.
[7] H. Yuk, B. Lu, S. Lin, K. Qu, J. Xu, J. Luo, X. Zhao, *Nat. Commun.* **2020**, *11*, 4.
[8] Z. Jiang, B. Diggle, M. L. Tan, J. Viktorova, C. W. Bennett, L. A. Connal, *Adv. Sci.* **2020**, *7*, 2001379.
[9] Y. Li, Z. Wu, Y. Chen, S. Xian, Z. Hong, Q. Wang, Jiang, H. Yu, Y. Zhong, *Addit. Manuf.* **2024**, *85*, 104178.
[10] P. Minetola, A. Giubilini, *Prog. Addit. Manuf.* **2024**, *9*, 2273.
[11] M. Schouten, G. Wolterink, A. Dijkshoorn, D. Kosmas, S. Stramigioli, G. Krijnen, *IEEE Sens. J.* **2021**, *21*, 12900.
[12] A. Kalkal, S. Kumar, Kumar, R. Pradhan, M. Willander, G. Packirisamy, S. Kumar, B. D. Malhotra, *Addit. Manuf.* **2021**, *46*, 102088.
[13] H. Sun, J. Zettl, N. Willenbacher, *Addit. Manuf.* **2023**, *78*, 103872.
[14] M. M. Mohammadi, S. Choi, Koirala, G. C. Jayatilaka, N. Ghousifam, H. Celio, M. Tehrani, *Addit. Manuf. Lett.* **2022**, *3*, 100061.
[15] F. Hong, B. Lampret, C. Myant, S. Hodges, D. Boyle, *Addit. Manuf.* **2023**, *70*, 103546.
[16] O. F. Emon, F. Alkadi, M. Kiki, J. W. Choi, *Addit. Manuf. Lett.* **2022**, *2*, 100027.
[17] S. Marion, T. Joffre, J. Jaxel, F. Pigeonneau, *Addit. Manuf.* **2023**, *79*, 103939
[18] H. G. Kim, S. Hajra, D. Oh, N. Kim, H. J. Kim, *Compos. Part B Eng.* **2021**, *222*, 109079.
[19] M. Maurizi, J. Slavic, F. Cianetti, M. Jerman, J. Valentincic, A. Lebar, M. Boltezar, *Sensors (Switzerland)* **2019**, *19*, 2661.
[20] B. Urasinska-Wojcik, N. Chilton, Todd, C. Elsworthy, M. Bates, G. Roberts, G. J. Gibbons, *Addit. Manuf.* **2019**, *29*, 10077.
[21] M. Lalegani Dezaki, R. Sales, A. Zolfagharian, H. Yazdani Nezhad, M. Bodaghi, *Int. J. Adv. Manuf. Technol.* **2023**, *128*, 4207.
[22] F. Grønborg, T. G. Zsurzsan, A. E. Daugaard, J. Spangenberg, D. B. Pedersen, *Addit. Manuf. Lett.* **2022**, *3*, 100088.
[23] J. Oprel, G. Wolterink, J. Schilder, G. Krijnen, *Addit. Manuf.* **2023**, *73*, 103674.
[24] G. D. Liu, C. H. Wang, Z. L. Jia, K. X. Wang, *J. Micromech. Microeng.* **2021**, *31*, 065005.
[25] L. Y. W. Loh, U. Gupta, Y. Wang, C. C. Foo, J. Zhu, W. F. Lu, *Adv. Eng. Mater.* **2021**, *23*, 2170018.
[26] T. Košir, J. Slavič, *Addit. Manuf.* **2023**, *73*, 103699.
[27] G. Stano, S. M. A. I. Ovy, J. R. Edwards, M. Cianchetti, G. Percoco, Y. Tadesse, *Int. J. Adv. Manuf. Technol.* **2023**, *124*, 467.
[28] Y. Jiang, M.d. N. Islam, R. He, X. Huang, F. Cao, R. C. Advincula, N. Dahotre, Dong, H. F. Wu, W. Choi, *Adv. Mater. Technol.* **2023**, *8*, 2200492.
[29] M. R. Khosravani, T. Reinicke, *Sensors Actuators, A Phys* **2020**, *305*, 111916.
[30] N. Qureshi, V. Dhand, S. Subhani, R. S. Kumar, N. Raghavan, S. Kim, J. Doh, *Adv. Mater. Technol.* **2024**, *9*, 2400250.
[31] K. Angel, H. H. Tsang, S. S. Bedair, G. L. Smith, N. Lazarus, *Addit. Manuf.* **2018**, *20*, 164.
[32] M. J. Kim, M. A. Cruz, S. Ye, A. L. Gray, G. L. Smith, N. Lazarus, C. J. Walker, H. H. Sigmarsson, B. J. Wiley, *Addit. Manuf.* **2019**, *27*, 318.
[33] N. Lazarus, S. S. Bedair, S. H. Hawasli, M. J. Kim, B. J. Wiley, G. L. Smith, *Adv. Mater. Technol.* **2019**, *4*, 1900126.
[34] J. Zhan, T. Tamura, X. Li, Z. Ma, M. Sone, M. Yoshino, S. Umezu, H. Sato, *Addit. Manuf.* **2020**, *36*, 101556.
[35] N. Lazarus, J. B. Tyler, J. A. Cardenas, B. Hanrahan, H. Tsang, S. S. Bedair, *Addit. Manuf.* **2022**, *55*, 102793.
[36] S. Akin, C. Nath, M. B. G. Jun, *ACS Appl. Electron. Mater.* **2023**, *5*, 5164.
[37] R. Melentiev, A. Lagerweij, G. Lubineau, *Smart Mater. Manuf.* **2023**, *2*, 100043.
[38] T. Ludergnani, G. Fredi, L. Malagutti, A. Balbo, A. Dorigato, F. Mollica, V. Mazzanti, *Macromol. Mater. Eng.* **2023**, *308*, 17.
[39] G. Stano, A. Pavone, M. A. Jafor, K. Matalgah, G. Percoco, T. J. Fleck, *Virtual Phys. Prototyp.* **2024**, *19*, 2331153.
[40] N. A. Mohd Radzuan, A. B. Sulong, J. Sahari, *Int. J. Hydrogen Energy* **2017**, *42*, 9262.
[41] F. Daniel, N. H. Patoary, A. L. Moore, L. Weiss, A. D. Radadia, *Int. J. Adv. Manuf. Technol.* **2018**, *99*, 1215.
[42] A. K. Bose, X. Zhang, D. Maddipatla, S. Masihi, M. Panahi, B. B. Narakathu, B. J. Bazuin, J. D. Williams, M. F. Mitchell, M. Z. Atashbar, *IEEE Sens. J.* **2020**, *20*, 12652.
[43] E. MacDonald, R. Wicker, *Science* **2016**, *353*. https://doi.org/10.1126/science.aaf2093
[44] D. A. Sepulveda-Navarrete, S. Gutierrez, A. Lopes, J. I. Rome, V. K. Goyal, D. Espalin, *Addit. Manuf.* **2023**, *73*, 103662.
[45] N. Sayah, D. E. Smith, *J. Compos. Sci.* **2024**, *8*, 246.
[46] N. Sayah, D. E. Smith, *Polymers (Basel)* **2022**, *14*, 5107.
[47] E. Macdonald, R. Salas, D. Espalin, M. Perez, E. Aguilera, D. Muse, R. B. Wicker, *IEEE Access* **2014**, *2*, 234.